ELSEVIER

Journal of Volcanology and Geothermal Research 101 (2000) 199–209

Journal of volcanology and geothermal research

www.elsevier.nl/locate/jvolgeores

Locating tremor and shock sources recorded at Bromo Volcano

E. Gottschämmer[a,*], I. Surono[b]

[a]*Geophysical Institute, University of Karlsruhe, Hertzstrasse 16, 76187 Karlsruhe, Germany*
[b]*Volcanological Survey of Indonesia, Bandung, Indonesia*

Accepted 20 August 1999

Abstract

During a phase of high eruptive activity, as well as high tremor activity, seismic signals were recorded at Bromo Volcano (East Java) for almost three months in 1995. The signals generated by the volcano cover a broad frequency range including long period signals with frequencies between 10 and 100 mHz, tremor signals at about 5 Hz and volcanic shocks with frequencies up to 25 Hz. Seismic signals from volcanoes, especially tremors, have been classified and categorized in different ways, but interpretation has always been limited by the difficulties in determining even approximate source locations. Volcanic tremor lacks an emergent first onset, while the complex structure of the volcano makes it difficult to determine other phases from shock signals than first arrivals.

If the volcanic signal has been recorded in at least two stations, the location of its seismic source can be estimated using a grid search method if we assume the source radiates isotropically in a homogeneous medium.

Applying the grid method to data recorded at Mt. Bromo, we determine the locations of the sources of tremor and shock signals. The sources for both types of signals are located in the northwestern part of the crater, near the open vent and also near the source of long period signals (Gottschämmer, 1999. Annal. Geofis. 42 465–481).

Keywords: volcano seismology; volcanic tremor; determination of source locations

1. Introduction

Mount Bromo, a member of the chain of active volcanoes stretching across Java, is situated inside Tengger Caldera at the northern end of the national park which also encompasses Semeru, the highest mountain on Java, 20 km to the south. Mount Bromo, the only active volcano inside the caldera, is a small pyroclastic cone with a wide crater, 700 m in diameter.

At Mt. Bromo eruptive episodes have alternated with decades of quiescence. Since 1804 more than 50 eruptions have been observed (GVN, March 1995). Nevertheless, Mt. Bromo has only rarely been the object of scientific investigations.

After a decade of quiescence, Mt. Bromo's recent activity began in March 1995. The level of activity increased in September 1995, including major ash cloud eruptions. The eruptive activity was accompanied by high levels of tremor (GVN, October 1995).

Volcanic tremor signals have recently become a subject of great interest, and various source mechanisms have been suggested. Depending on the spectral content of the signal, a tremor is divided into harmonic tremor and non-harmonic tremor. Spectra of

* Corresponding author. Tel.: + 49-721-6084592; fax: + 49-721-71173.

E-mail address: gottschaemmer@physik.uni-karlsruhe.de (E. Gottschämmer).

0377-0273/00/$ - see front matter
PII: S0377-0273(00)00171-2

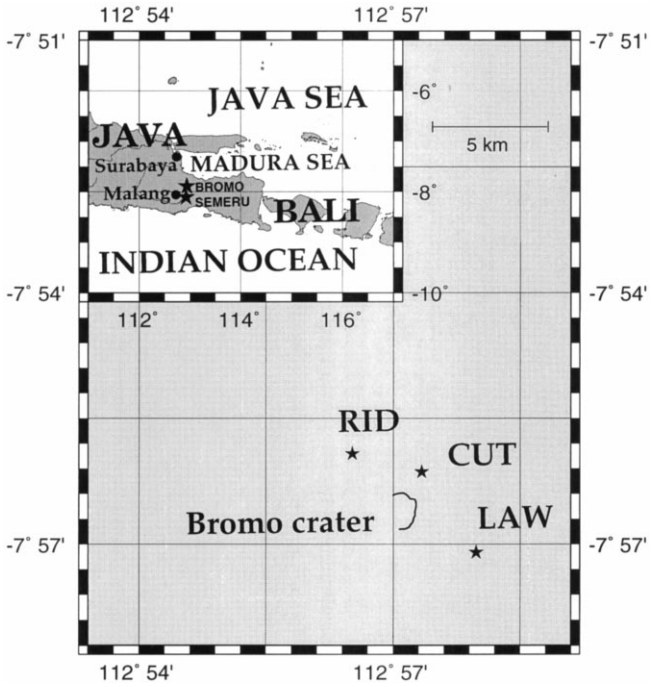

Fig. 1. Map showing the positions of the stations RID, CUT and LAW (*) at Mt. Bromo.

harmonic tremors have sharp peaks at well-defined frequencies and, in certain cases, contain up to 11 overtones (Schlindwein et al., 1995). Some investigators suggest that these signals are produced by the resonance of a pipe or a crack (Aki et al., 1977; Dahm, 1991; Schlindwein et al., 1995) or by fluid motion (Hellweg, 2000 – this issue). Non-harmonic tremor, such as that recorded at Bromo Volcano, has a broad spectrum with no notable peaks (Mohnen and Schick, 1996). Physical models proposed for the source of this type of tremor include oscillating (Chouet et al., 1997) or exploding gas bubbles (Ripepe et al., 1996). However, it is difficult to determine the location of the tremor source. Attempts have been made to find the source location for harmonic tremor signals using polarization analysis (Seidl and Hellweg, 1991; Benoit and McNutt, 1997). These methods can not be applied to non-harmonic tremor as they only work for narrowband signals.

The situation for volcanic shocks is similar. The source mechanism for these signals is assumed to be similar to that of very small earthquakes like rock fractures (Fadeli, 1991; Schick, 1991). It is difficult to locate sources using normal seismological methods because phases other than the first onset can rarely be identified.

A grid search over some location-dependent parameter measured from the seismogram can provide a mean for determining the location of the source for both types of volcanic signals.

2. Seismic experiment

From September–December 1995 three seismic stations (LAW, RID, CUT) were deployed on Bromo Volcano between 0.5 and 2.5 km from the crater rim (Fig. 1). Each of the stations was equipped with a GURALP CMG-3T broadband seismometer (three components) and a Lennartz MARS-88/OD data acquisition system. When the sampling frequency is set to 62.5 Hz, this system has a flat response with respect to ground velocity from the corner frequency of the seismometer, 0.0083 Hz (120 s period) to the corner frequency of the anti-aliasing filter, 25 Hz. Each station was also equipped with a GPS time signal receiver. Data were recorded continuously from 21 September to 13 December

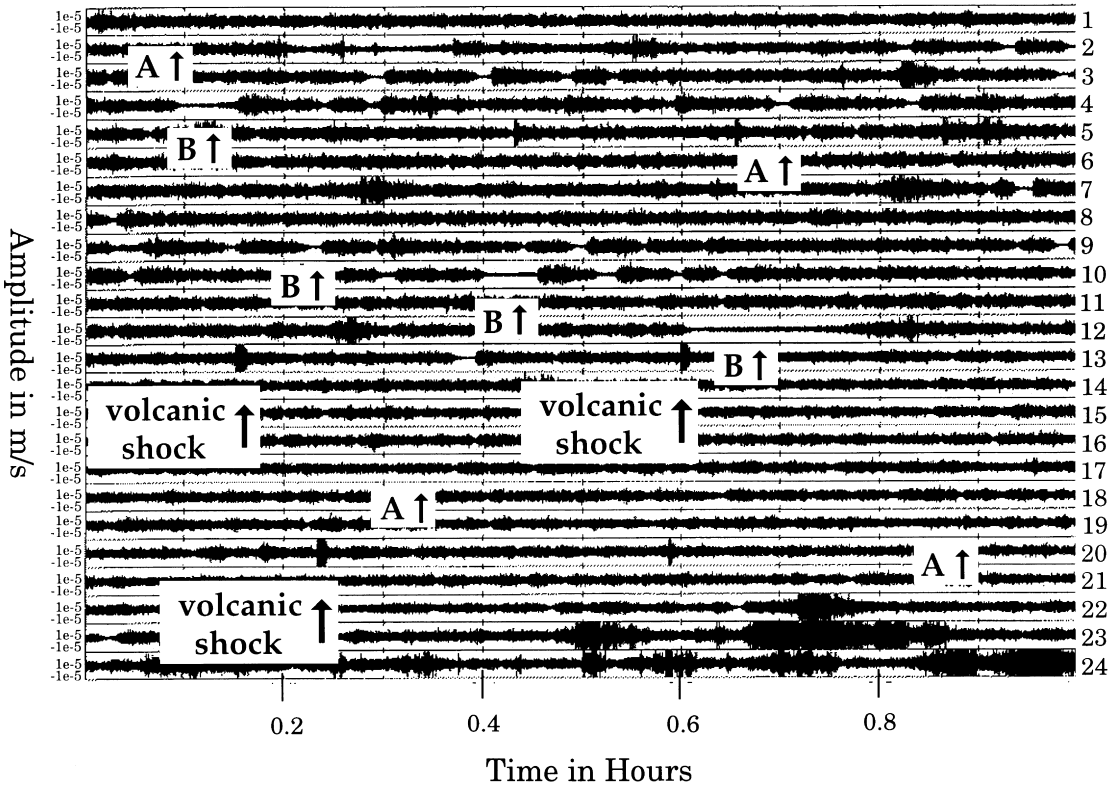

Fig. 2. Velocity seismogram for 4 November, station RID, *Z*-component. Each trace shows the recording for 1 h. The top trace starts at 00:00 UT which was 07:00 local time (LT). High tremor amplitudes (phase A) alternate with low amplitudes (phase B). The amplitudes of the volcanic shocks are clipped in this figure. Slowly increasing and decreasing amplitudes between 21:00 and 00:00 UT are caused by cars passing close by the station when people drove to the crater to watch the sunrise.

accumulating a total of 15 GB of data. This study focuses on the analysis of data from only four days (14 and 15 October, 12 and 16 November). The experiment was carried out jointly by the Volcanological Survey of Indonesia, Bandung, the University of Leeds, UK, the University of Grenoble, France and the University of Stuttgart, Germany.

3. The data

The most conspicuous feature in the data is the tremor, which consists of two phases. Intervals with almost constantly high amplitude tremor (phase A) that alternate with intervals in which the tremor amplitude is nearly constant but low (phase B). In Fig. 2 the two phases can be distinguished. Despite the difference in amplitude, the spectral content of the two phases is the same, showing a broad spectral peak of several Hertz bandwidth and a maximum around 5 Hz (Gottschämmer, 1999). Each type of tremor phase may last from 10 min to more than a day. Transitions between phases happen rapidly, taking only several minutes.

Superimposed on the recordings of the tremor activity are volcanic shocks. On the average they occur two or three times per day. Fig. 2 gives an example. Volcanic shocks are signals with a short duration and usually have larger amplitudes than the tremor. It is suggested that volcanic shocks are produced by fracturing or cracking within the rocks (Fadeli, 1991; Schick, 1991) or by gas explosions (Schick, 1991). Apart from ash cloud eruptions which have been reported by people involved in the

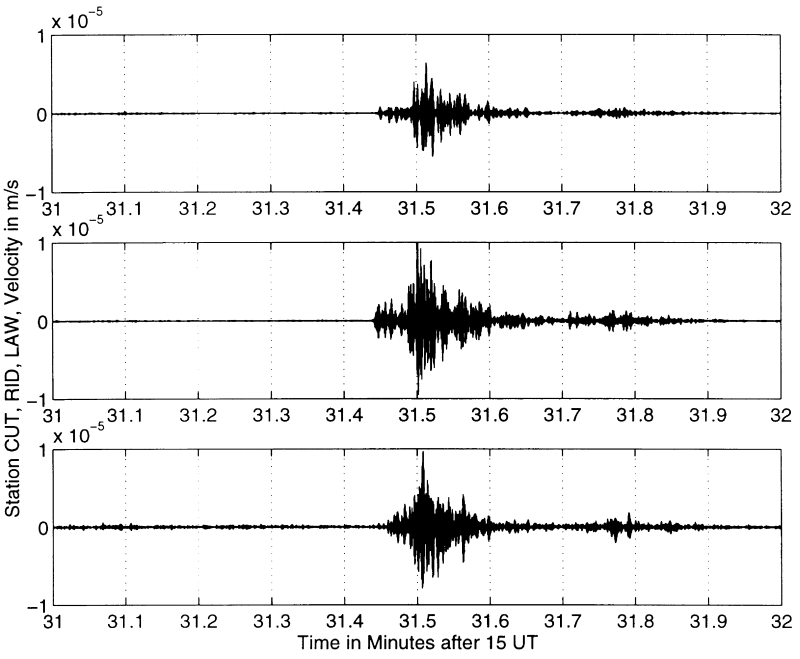

Fig. 3. Velocity seismograms for a volcanic shock on 12 November, stations LAW, RID and CUT (from top), *Z*-component. The time is displayed in minutes after 15:00 UT. The seismograms have been bandpass-filtered from 20 to 25 Hz.

experiment (J. Neuberg, personal communication) no visual observations of external activity has been available to us.

4. The grid method

A volcanic tremor has no onsets that can be used to determine the location of its source. The onsets for volcanic shocks are often masked in the tremor, while later phases are missing or hard to recognize, making them difficult to locate. We developed a grid search method using location-dependent parameters measured from tremor or shock seismograms to determine locations of their sources. For this method, data must be available for at least two stations. The determination can be improved by using data from more stations. Several assumptions are necessary for applying the grid method. We must assume that waves are radiated from the source in the same way in all directions (isotropic radiation). Furthermore we assume that the medium between source and station is homogeneous with respect to the P-wave velocity *v*.

We define a uniform grid of $i \times j$ points over the region where we expect the source to be, with $i, j \approx 100$. The number and spacing of the grid points is determined by the desired resolution. For each grid point, the distance to each of the N stations is computed. Next, we calculate a single value A_{ij_n} (e.g. source time for volcanic shocks, emitted power of the source for volcanic tremor) for each grid point P_{ij} from the recordings of station n. The same computation is performed for all the other $N-1$ stations. In this way we assign N of the parameter A to each grid point. For the true source position these values should agree ($A_{ij_1} = A_{ij_2} = \ldots = A_{ij_N}$). If there is no grid point for which all values A_{ij_N} match, the resolution of the grid may not be fine enough or the assumptions of isotropic radiation and homogeneity may not be held. In that case, the approximate source position can be determined by the minimum of the standard deviation:

$$\sigma_{ij} = \sqrt{\frac{1}{N-1}\sum_{n=1}^{N}(A_{ij_n} - \bar{A}_{ij})^2},$$

where $\bar{A}_{ij}$ is the average over all A_{ij_n}.

The advantage of the grid search method is that

Table 1
Arrival times of several volcanic shocks B_1 to B_6 in seconds after the hours displayed in the first column for the three stations LAW, RID and CUT

Date, hour (UT)	No.	LAW	RID	CUT
14/10/95, 06	B_1	543.8	543.5	541.2
14/10/95, 10	B_2	1248.4	1248.0	1245.9
14/10/95, 13	B_3	202.4	201.9	200.2
12/11/95, 04	B_4	811.5	811.2	809.0
12/11/95, 15	B_5	1886.9	1886.5	1885.2
16/11/95, 10	B_6	2804.1	2803.8	2801.0

only one parameter needs to be determined for each station. For volcanic shocks, for example, the determination of the first onset is sufficient, and onsets from additional phases are not necessary. Problems occur, however, if the medium is inhomogeneous or anisotropic. In this case, the coordinates of the resulting source location may depend on the k parameters R_k, such as the P-wave velocity v, the depth z of the source or the absorption coefficient, κ, of the medium, used in the calculation of A_{ij}.

Therefore, the influence of each of the k parameters R_k must be analysed separately. Instead of searching for the minimum of the standard deviation in a two-dimensional space constructed using i and j, we must find the minimum in a space with $k + 2$ dimensions.

5. Applying the grid method to volcanic shocks

Volcanic shocks were recorded at Bromo Volcano during the entire deployment. On the average, two or three shock signals were recorded at all three stations each day. Fig. 3 shows velocity seismograms for a shock on 12 November (15:31–15:32 UT) for all three stations (vertical components). The data have been bandpass-filtered between 20 and 25 Hz in order to remove superimposed signals. The onsets of the signals can be clearly determined. The arrival times for this shock and five others listed in Table 1 are averaged over all components. We placed a grid of 100×100 points over the region around the crater of Mt. Bromo. If the distance from the grid point P_{ij} to a station is s_{ij}, the source time $t_{H_{ij}}$ can be calculated from the arrival time t_{arr} of the seismic wave at any station and the travel time $t_{\text{trav}_{ij}}$ between the source and the

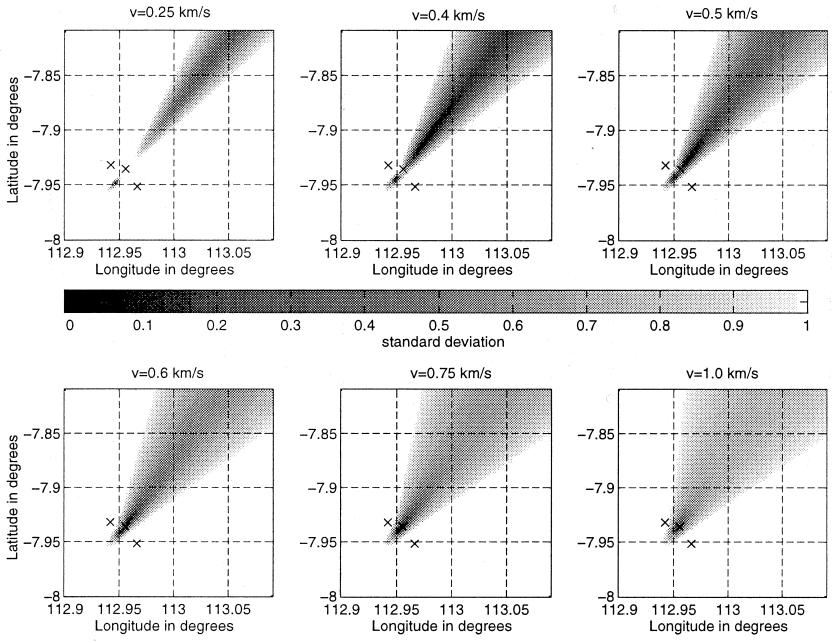

Fig. 4. Standard deviation σ_{ij} of source times $t_{H_{ij}}$ for all grid points P_{ij} calculated for different velocities. The picture in the top left corner is calculated for a velocity $v_{\text{guess}} = 0.25$ km/s. The velocity is increased up to 1 km/s in the picture in the lower right corner.

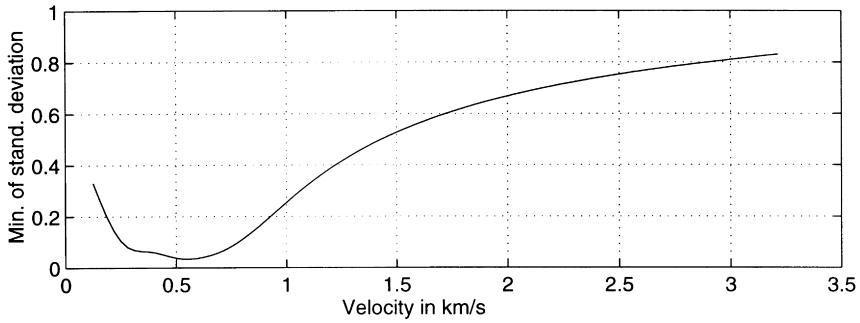

Fig. 5. Minimum of standard deviation shown in Fig. 4 for different velocities v_{guess}. The overall minimum of the standard deviation occurs at $v_{\text{guess}} = 0.56$ km/s.

station:

$$t_{\text{arr}} = t_{H_{ij}} + t_{\text{trav}_{ij}} = t_{H_{ij}} + \frac{s_{ij}}{v_{\text{guess}}} \tag{1}$$

$$\rightarrow t_{H_{ij}} = t_{\text{arr}} - \frac{s_{ij}}{v_{\text{guess}}}. \tag{2}$$

The source time can be calculated if we assume a seismic wave velocity v_{guess}.

The source time $t_{H_{ij}}$ is calculated for each station resulting in three source time values for each grid point. These three values can be compared by calculating a standard deviation σ_{ij} for every grid point P_{ij}. Fig. 4 shows the standard deviation of the source times for different velocities v_{guess} for shock B_4. The source is located where the standard deviation has a minimum, depicted by dark regions in Fig. 4. The source location and the value of the standard deviation depend on the value of the velocity used in the calculation. The minimum standard deviation is, therefore, taken from each plot in Fig. 4 and plotted as a function of the velocity v_{guess} (Fig. 5). The minimum standard deviation occurs when the velocity is $v_{\text{guess}} = 0.56$ km/s.

The depth of the shocks does not play an important role in the source location. Typically, volcanic shocks occur at shallow depths less than 5 or 6 km (Fadeli, 1991; GVN, November 1996; GVN, February 1997; GVN, April 1997). For these depths, source locations of the volcanic shocks determined using the grid search method only vary by several tens of meters.

After deciding on a velocity appropriate for all

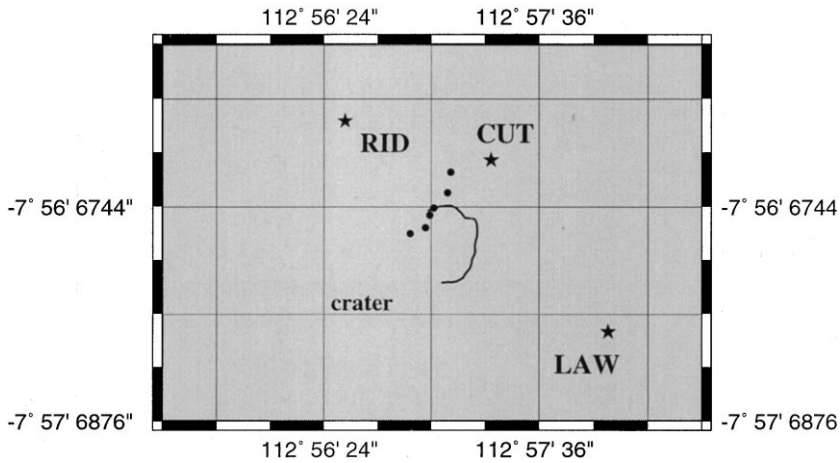

Fig. 6. Map showing sources of shock signals at Mt. Bromo. The positions of the sources are displayed by dots (●). The station locations are indicated by stars (*). The positions of the sources almost form a line. This line is parallel to the symmetry axis of the patterns in Fig. 4.

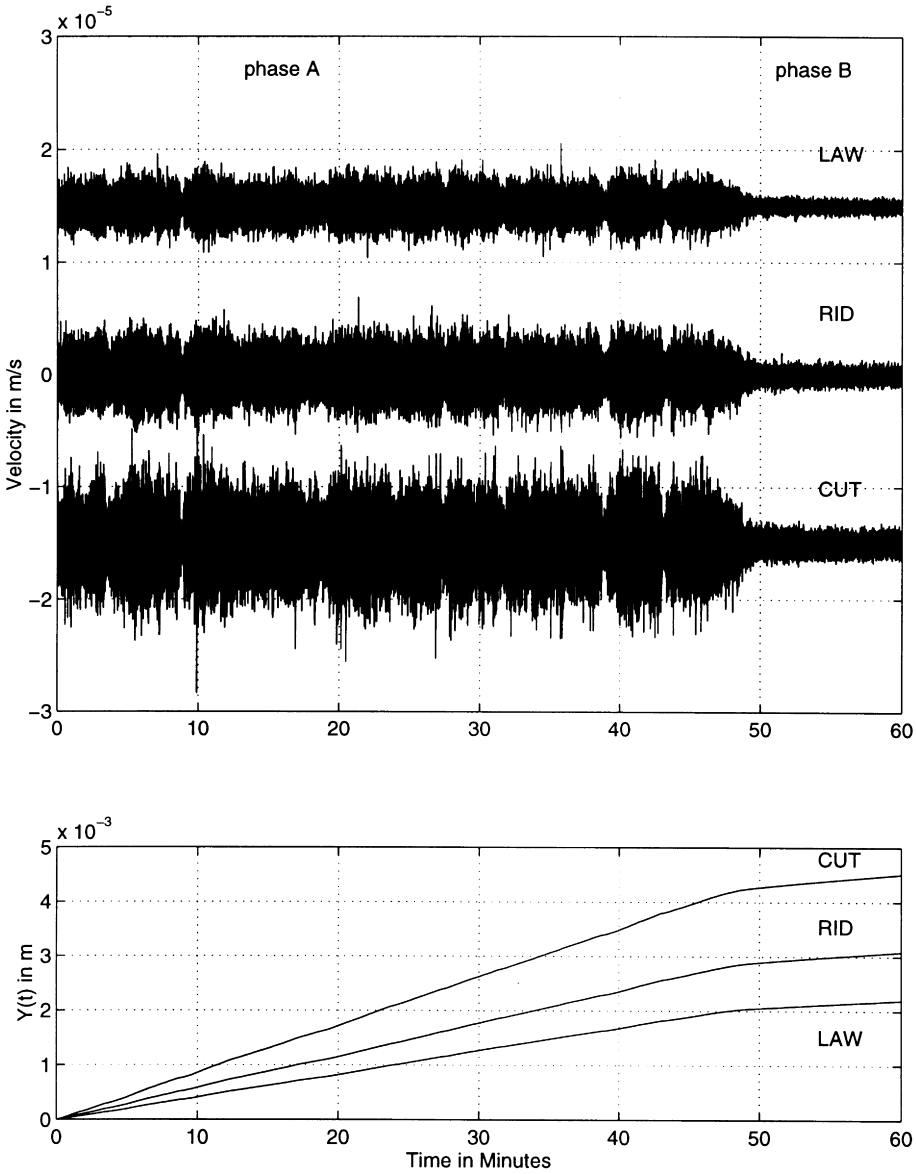

Fig. 7. Top: velocity seismograms for 17 October, 17:00–18:00 UT, stations LAW, RID and CUT (from top), *Z*-component. For the first 46 min phase A tremor can be seen. After a transition, of about 2 min, the tremor activity has shifted to phase B. Bottom: integrals $Y(t)$ of the seismograms shown above. The line with the highest slope belongs to station CUT where the amplitudes in the velocity seismogram have been highest. The middle and lower lines are calculated from the seismograms recorded at stations RID and LAW, respectively. The slope of the integral is nearly constant within either phase A or B. The respective slopes are fit with straight lines not shown in the figure.

shock signals listed in Table 1, we calculated their source locations. They are plotted in Fig. 6 on a map of Mt. Bromo. All shocks are located near the northwestern edge of the crater and form a nearly straight line. This line is essentially parallel to the 'valleys' of low standard deviation in the plots of Fig. 4. These valleys are an artefact of the network configuration and show that the resolution of the grid search is smaller in this direction than in a direction perpendicular to it.

Table 2
Source coordinates for phase A and phase B tremor for a medium with no absorption ($\kappa = 0\ \mathrm{m}^{-1}$, third column) and including absorption ($\kappa = 3.1 \times 10^{-4}\ m^{-1}$, last column)

Date, time (UT)	Phase	Long./Lat. ($\kappa = 0\ \mathrm{m}^{-1}$)	Long./Lat. ($\kappa = 3.1 \times 10^{-4}\ \mathrm{m}^{-1}$)
14/10/95, 19–20	A	112.9480°W/−7.9430°S	112.9480°W/−7.9435°S
15/10/95, 12–13	A	112.9480°W/−7.9430°S	112.9480°W/−7.9435°S
15/10/95, 18–19	B	112.9460°W/−7.9430°S	112.9460°W/−7.9435°S
12/11/95, 06–07	A	112.9470°W/−7.9435°S	112.9470°W/−7.9440°S
12/11/95, 21–22	A	112.9475°W/−7.9410°S	112.9475°W/−7.9415°S
16/11/95, 07–08	A	112.9490°W/−7.9425°S	112.9490°W/−7.9425°S
16/11/95, 14–15	B	112.9500°W/−7.9430°S	112.9495°W/−7.9435°S

6. Application of the grid method to volcanic tremor

For a volcanic tremor that lacks clear onsets and phases (Neuberg and Wahyudi, 1991) the distance-dependent parameter for the grid search method is the power of the source. This parameter can be calculated from the seismograms. The energy E emitted by a seismic source is given by Schick and Schneider (1973) as:

$$E = 4\pi R^2 \rho v\, \mathrm{e}^{\kappa R} \int_{t_1}^{t_2} y^2\, \mathrm{d}t \qquad (3)$$

where R is the distance from the source to the receiver, ρ the density of the medium, κ the absorption coefficient, v the velocity of the waves and y the velocity amplitude of the recorded signal.

The power emitted by the source, $P = \mathrm{d}E/\mathrm{d}t$, is then:

$$P = 4\pi R^2 \rho v\, \mathrm{e}^{\kappa R} y^2. \qquad (4)$$

The velocity amplitude y itself oscillates between the maximum and the minimum value (e.g. $\pm 5 \times 10^{-6}$ m/s for phase A at station CUT, Fig. 7), but the envelope of this signal remains nearly constant over a long interval. Therefore, the velocity amplitude y is substituted by $\bar{y}$, the average of the absolute value of y. Over a period of 1 h, during which the tremor signal showed either phase A or phase B activity, $\bar{y}$ is calculated as follows.

The integral $Y(t) = \int_{t_1}^{t_2} y^2\, \mathrm{d}t$ is computed and plotted as a function of the time t (Fig. 7). The seismograms from which the integrals were calculated are shown above and were chosen so that they included no disturbing signals such as shocks or long period signals. $Y(t)$ rises linearly during an interval of either tremor A or B but with different slope. Each rise can be fitted with a straight line, the slope of which gives the average velocity amplitude $\bar{y}(t)$. This value is then substituted for $y(t)$ in Eq. (4)

The floor of the caldera is mainly sand, so we use $\rho = 2000\ \mathrm{kg/m}^3$ (wet sand (Kuchling, 1991)) and assume that the velocity is 1 km/s. Initially, we take the absorption κ to be zero.

For each grid point and each seismic station we now calculate the power which would have been emitted if the source was located at that point. In this way, we get three power values for each grid point, according to the three stations. The source coordinates are then calculated using the grid search method: we find the grid point at which the standard deviation shows a minimum. This grid point represents the source location if the medium is homogeneous and the source radiates isotropically.

Table 2 (third column) shows the coordinates for the tremor source during phase A and during phase B for $\kappa = 0$. The sources are located within a 300 m north–south and 400 m east–west range. It is not possible to distinguish between a source location for phase A and phase B tremors. The power emitted by the volcanic source, however, is different for the two phases. It varies between 31 and 90 W during phase A and lies between 3 and 5 W during phase B.

Up to this point absorption has not been taken into account. Usually though, in volcanic areas, absorption of energy is high due to unconsolidated rocks, ash and sand. Especially at Bromo Volcano, which is embedded in a caldera filled with sand, absorption

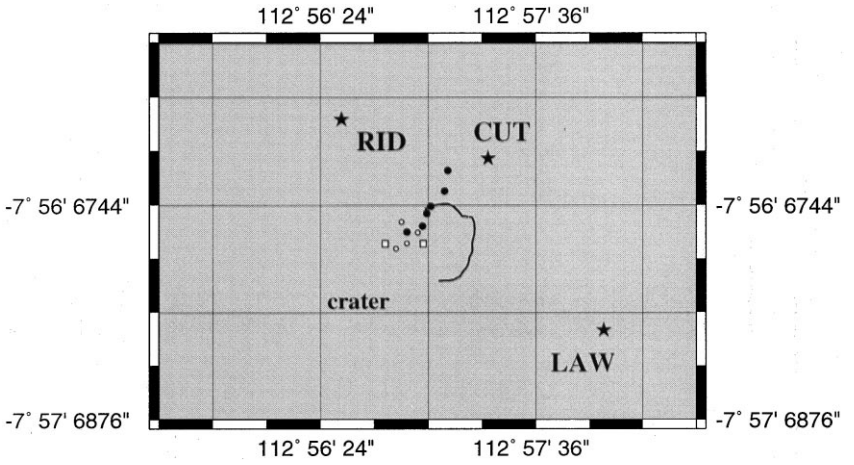

Fig. 8. Map showing the position of the sources of the tremor signals which are displayed by circles (○, phase A) and squares (□, phase B). Source positions are located in the northwestern area of the crater. Also included in this figure are the source positions of the shock signals from Fig. 6 (●).

has to be considered. For the absorption coefficient we can write:

$$\kappa = \frac{\pi}{Q\lambda_0}. \tag{5}$$

It depends on the dominant wavelength, λ_0 which can be expressed as:

$$\lambda_0 = \frac{v_{\text{phase}}}{f_0} \tag{6}$$

with a dominant frequency f_0, which for the tremor signals lies around 5 Hz and the phase velocity v_{phase}.

The absorption coefficient also depends on the quality factor Q which we assume to be 50 (Del Pezzo and Patané, 1992).

Inserting Eq. (6) into Eq. (5) gives:

$$\kappa = \frac{\pi f_0}{Q v_{\text{phase}}}. \tag{7}$$

We assume a phase velocity of 1 km/s. The absorption coefficient κ is therefore 3.1×10^{-4} m^{-1}.

The source coordinates determined using the absorption coefficient κ differ only slightly from the calculations for which κ was set to zero (Table 2, last column). Fig. 8 shows the locations of the tremor sources calculated using $\kappa = 3.1 \times 10^{-4}\, m^{-1}$. Again, phase A tremor sources which are displayed by circles cannot be separated from phase B tremor sources displayed by squares. The sources of both types of tremor are located close to the northwestern part of the crater rim with a maximum separation of 400 m. For comparison, the sources of the tremor signals are also included in this figure as black dots. Depending on the distance between the station and the source, the power radiated by the source must be 60–80% higher in this case than when $\kappa = 0$.

If we assume a different wave velocity, the source locations are not affected. When velocities are unreasonably high or low, the power of the source changes, but the source coordinates determined by the grid search method stay the same. Changing the depth of the tremor sources has slightly more effect on the source location. Nonetheless, when the source depth changes within reasonable limits, for example by several hundred meters (Schick and Riuscetti, 1973; Benoit and McNutt, 1997), the source location is not affected at all.

7. Interpretation

Using the grid search method we determined that the sources of both the tremor and shock signals are located in the northwestern part of Mt. Bromo's active crater. The individual sources of the shock signals are nearly aligned and point towards the region where the

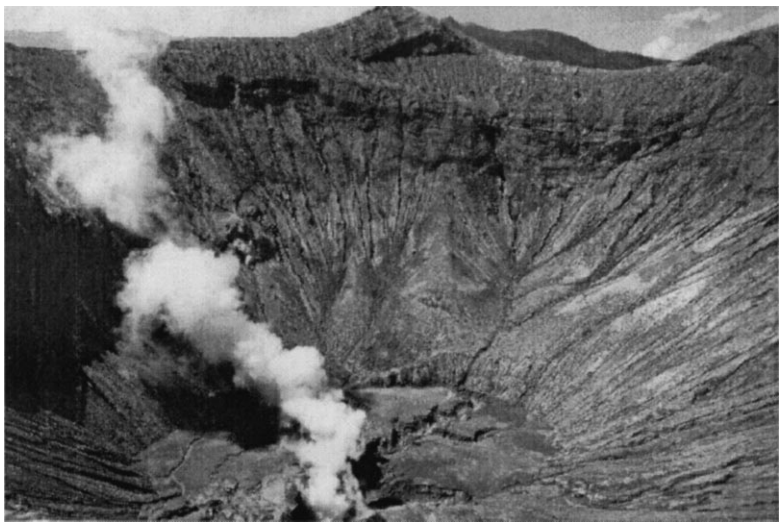

Fig. 9. View from the rim of Mt. Bromo into the crater. Viewing direction is towards the southeast. In the northwestern part of the crater, steam rises from the vent. An eruption cloud of Semeru can be seen above the crater rim at top right.

tremor sources are located. Shock signals are believed to be generated by the formation of fissures or cracks in the conduit walls when the pressure inside the conduit exceeds a limiting value (Fadeli, 1991; Schick, 1991). Thus, the location of the shock signal sources may indicate the position of the conduit.

The tremor signals at Mt. Bromo cover a broad frequency range. Thus, they cannot be generated by a single oscillator as suggested for harmonic tremor signals (Schlindwein et al., 1995). Due to the lack of magmatic eruptions at Mt. Bromo, it is also impossible that tremor signals at Mt. Bromo originate from oscillating bubbles within the magma as suggested by Chouet et al. (1997) for Stromboli. Eruptive activity at Mt. Bromo is dominated by ash eruptions. Therefore, it is more likely that the tremor signals at Mt. Bromo are created by the flow of gases and steam through an irregularly shaped conduit that produces a large variety of frequencies.

From the crater rim, an open vent can be seen at the northwestern section of the crater (Fig. 9), the area which corresponds to the locations of the sources of volcanic tremor. This is another indication that the tremor signals are connected to the venting of gas and steam. The source of long-period tilt signals is located in the same region (Gottschämmer, 1999).

8. Discussion

The grid search method allows the determination of source locations by comparing the values of a single distance-dependent parameter calculated for different seismic stations. With a limited data set, the method is based on simplifying assumptions that the medium through which the waves travel is homogeneous and radiation is isotropic. The results are influenced by the assumptions made about the medium and the radiation of the source. If they are not correct, the method produces biased results. Unfortunately, in a volcano the medium is unlikely to be isotropic and homogeneous even over short distances.

A second effect is caused by the positions of the stations and by their small number. For best results, three stations should be deployed in an equilateral triangular array embedding the source in their middle. When stations are deployed in a line, the resolution is good for waves arriving in the direction of the line but poor for waves travelling perpendicular to it. At Bromo, the station distribution was not ideally chosen regarding the source position, due to restrictions caused by the accessibility of the area. The stations are deployed in a triangle of which the longest side extends from NW to SE. With this distribution, the resolution is better in the NW–SE direction than in the

NE–SW direction. This also affects the source determination of the tremor signals. The source locations found with the grid search method almost form a line from NE to SW. In this direction, though, the determination is less restrictive than in the direction perpendicular to it.

Acknowledgements

We wish to thank Dr W. Zürn for many helpful discussions, for suggesting several improvements and for critically reading the manuscript. We are grateful to Prof R. Schick who also read the manuscript and helped us very much with his comments and suggestions to improve the paper. Special thanks are due to Dr J. Neuberg for fruitful discussions and, together with D. Francis, for making the data available and for helping with the data processing. Furthermore, we would like to thank H. Triastuty, A. Susilo, Prof E. Wielandt, Dr R. Widmer-Schnidrig, M. Hellweg and an anonymous reviewer for their constructive comments. This project could not have been realized without the assistance during the fieldwork of many members from the Universities of Leeds (UK), Grenoble (France) and Stuttgart (Germany) and members of the Volcanological Survey of Indonesia (Bandung). The project was financially supported by the European Commission, Bruxelles.

References

Aki, K., Fehler, M., Das, S., 1977. Source mechanism of volcanic tremor: fluid-driven crack models and their application to the Kilauea eruption. J. Volcanol. Geotherm. Res. 2, 259–287.

Benoit, J.P., McNutt, S.R., 1997. New constraints on source processes of volcanic tremor at Arenal Volcano, Costa Rica, using broadband seismic data. Geophys. Res. Lett. 24, 449–452.

Chouet, B., Saccarotti, G., Martini, M., Dawson, P., De Luca, G., Milana, G., Scarpa, G., 1997. Source and path effects in the wave fields of tremor and explosions at Stromboli Volcano. J. Geophys. Res. 102 (B7), 15129–15150.

Dahm, T., 1991. Eigenvibrations of magma-filled dyke systems with complex geometry. Volcanic Tremor Magma Flow, 97–114.

Del Pezzo, E., Patané, D., 1992. Coda Q dependence on time, frequency and coda duration interval at Mt. Etna, Sicily. Volcanic Seismol., 109–119.

Fadeli, A., 1991. Location of seismic sources of Merapi (Central Java) with impulsive character. Volcanic Tremor Magma Flow, 137–148.

Gottschämmer, E., 1999. Volcanic tremor associated with eruptive activity at Bromo Volcano. Annal. Geofis. 42, 465–481.

Hellweg, M., 2000. Physical models for the source of Lascar's harmonic tremor. J. Volcanol. Geotherm. Res. 101, 183–198.

Kuchling, H., 1991. Taschenbuch der Physik, Verlag Harri Deutsch, Thun und Frankfurt am Main, 13. korr. Auflage.

Mohnen, J.U., Schick, R., 1996. The spatial amplitude distribution of volcanic tremor at Stromboli Volcano (Italy). Annal. Geofis. 39, 361–375.

Neuberg, J., Wahyudi, P.S., 1991. Study on characteristics and origin of volcanic seismic signals. Volcanic Tremor Magma Flow, 149–163.

Ripepe, M., Poggi, P., Braun, T., Gordeev, E., 1996. Infrasonic waves and volcanic tremor at Stromboli. Geophys. Res. Lett. 23, 181–184.

Schick, R., 1991. Volcanic activity parameters. Volcanic Tremor Magma Flow, 183–188.

Schick, R., Riuscetti, M., 1973. An analysis of volcanic tremors at South Italian volcanoes. Z. Geophys. 39, 247–262.

Schick, R., Schneider, G., 1973. Physik des Erdkörpers. Ferdinand Enke, Stuttgart.

Schlindwein, V., Wassermann, J., Scherbaum, F., 1995. Spectral analysis of harmonic tremor signals at Mt. Semeru Volcano, Indonesia. Geophys. Res. Lett. 22, 1685–1688.

Seidl, D., Hellweg, M., 1991. Volcanic tremor recordings: polarization analysis. Volcanic Tremor Magma Flow, 31–46.

Smithsonian Bulletin of Global Volcanism Network (GVN), 1995. Tengger Caldera (Bromo) SO_2 and tremor. 20 (3).

Smithsonian Bulletin of Global Volcanism Network (GVN), 1995. Tengger Caldera (Bromo) ash plume and tremor. 20 (10).

Smithsonian Bulletin of Global Volcanism Network (GVN), 1996. Pacaya (Guatemala) eruption on 11 November drops over 3.5 cm of ash. 21 (11).

Smithsonian Bulletin of Global Volcanism Network (GVN), 1997. Rabaul (Papua New Guinea) occasional stronger explosions and a tilt reversal. 22 (2).

Smithsonian Bulletin of Global Volcanism Network (GVN), 1997. Vesuvius (Italy) low seismicity prevails after March–May earthquake swarm. 22 (4).